

# Photopion reactions on deltas preexisting in nuclei

A. Fix

*Tomsk Polytechnic University, 634004 Tomsk, Russia*

I. Glavanakov, Yu. Krechetov

*Nuclear Physics Institute, 634050 Tomsk, Russia*

February 9, 2008

## Abstract

Reactions  $A(\gamma, \pi^+ p)$  are considered to proceed through the formation of  $\pi^+ p$  pairs on  $\Delta$  constituents in nuclei. We develop the nonrelativistic operator of  $\gamma\Delta^{++} \rightarrow \pi^+ p$  process in an arbitrary frame. The calculated cross section of  $^{12}C(\gamma, \pi^+ p)$  reaction is compared to the existing experimental data.

The role of isobars as nuclear constituents was a topic of a large body of research over a long time (a comprehensive review can be found in Refs.[1, 2]). There is a convincing evidence that a small admixture of internally excited nucleons always presents in nuclei. Since these virtual excitations, proceeding during the collisions  $NN \rightarrow N^*N(N^*N^*)$ , are more intensive at the large relative momenta of nucleons, the isobar configurations are assumed to be responsible for high momentum components of nuclear wave functions. Therefore, they can manifest themselves in nuclear reactions with large momentum transfers.

However, more direct way to demonstrate the existence of isobar constituents in nuclei as well as to gain a better insight into their dynamical properties is to study the so-called isobar knock-out processes [3]. In this regard, the  $A(\gamma, \pi^+ p)$  reactions, which can be interpreted merely as absorption of incoming photon on  $\Delta^{++}$  performed in a target nucleus followed by its real decay into  $\pi^+ p$  pair, are the most attractive ones. The main advantage of this channel is that it is free of any influence of direct photoproduction mechanism, in contrast to the  $A(\gamma, \pi^+ n)$  reaction, where the contribution of a preexisting  $\Delta^+$  will be overwhelmed by the  $\Delta^+$  creation on a quasifree proton in  $\gamma p \rightarrow \Delta^+ \rightarrow \pi^+ n$  process.

To date, only one exclusive measurement of  $A(\gamma, \pi^+ p)$  reaction has been reported in Ref.[4], where the results of the first comparative studies of  $^{12}C(\gamma, \pi^+ n)$  and  $^{12}C(\gamma, \pi^+ p)$  channels are presented. While the  $^{12}C(\gamma, \pi^+ n)$  cross section is dominated by the quasifree mechanism, the higher order FSI (Final State Interaction) processes involving also charge exchange are assumed to be the source of the  $^{12}C(\gamma, \pi^+ p)$  reaction yield. The latter assumption is, however, not undoubtedly confirmed by a calculation performed within the Valencia model (VM) [5], which markedly underestimates the data.

In this paper we want to explain the observed  $^{12}C(\gamma, \pi^+ p)$  cross section, at least partially, as a signature of the  $\Delta^{++}$  admixture in  $^{12}C$  ground state.

The starting point of our discussion is the elementary  $\gamma\Delta^{++} \rightarrow \pi^+ p$  amplitude, which we need as input for a nuclear calculation. It is schematically shown in Fig.1, where the energies and the momenta of participating particles are also labeled. The matrix element is constructed in analogy with one-particle exchange model. The relevant diagrams are depicted in Fig.1(a-d). We restrict ourselves to nonrelativistic limit keeping only terms up to the order  $(p/M)^2$ . The  $\pi N \Delta$  vertex is

$$\Gamma_{\pi N \Delta} = -i \frac{f_\Delta}{m_\pi} F_\pi(q_\mu^2) (\vec{\sigma}_{N\Delta} \cdot \vec{q}_{\pi N}) , \quad (1)$$

where  $\vec{q}_{\pi N} = (\vec{q}M_N - \vec{p}_N E_\pi)/(M_N + E_\pi)$  is the relative momentum in  $\pi N$  system. The transition spin operator  $\vec{\sigma}_{N\Delta}$  is defined by its reduced matrix element

$$\langle \frac{1}{2} \| \sigma_{N\Delta} \| \frac{3}{2} \rangle = -2 . \quad (2)$$

For the  $\pi N \Delta$  coupling constant we take the value  $f_\Delta^2/4\pi = 0.37$  obtained from the  $\Delta$  decay. It is generalized to the off-shell region by the conventional monopole form factor

$$F_\pi(q_\mu^2) = \frac{\Lambda^2 - m_\pi^2}{\Lambda^2 - q_\mu^2} \quad (3)$$

with a cut-off mass  $\Lambda = 1$  GeV and  $q_\mu$  being the pion 4-momentum.

For the nucleon and isobar currents the following expressions are used

$$\vec{j}_N = \frac{e}{2M_N} [e_N(\vec{p}_N + \vec{p}'_N) + \mu_N i(\vec{\sigma}_N \times \vec{k})] , \quad (4)$$

$$\vec{j}_\Delta = \frac{e}{2M_\Delta} [e_\Delta(\vec{p}_\Delta + \vec{p}'_\Delta) + \mu_\Delta i(\vec{\sigma}_\Delta \times \vec{k})] . \quad (5)$$

Here  $\vec{p}_N$  ( $\vec{p}_\Delta$ ) and  $\vec{p}'_N$  ( $\vec{p}'_\Delta$ ) are the incoming and outgoing nucleon (isobar) momenta, respectively. The charge and the magnetic moment of proton and  $\Delta^{++}$  are

$$e_p = 1 , \quad \mu_p = 2.79 \text{ n.m.} , \quad e_{\Delta^{++}} = 2 , \quad \mu_{\Delta^{++}} = -2.3 \text{ n.m.} , \quad (6)$$

where the value of  $\mu_{\Delta^{++}}$  was obtained in [6] within a bootstrap model. The spin operators  $\vec{\sigma}_N$  and  $\vec{\sigma}_\Delta$  have the following normalization

$$\langle \frac{1}{2} \| \sigma_N \| \frac{1}{2} \rangle = \sqrt{6} , \quad \langle \frac{3}{2} \| \sigma_\Delta \| \frac{3}{2} \rangle = 2\sqrt{15} . \quad (7)$$

After taking together all terms depicted in Fig.1(a-d), it is convenient to split the resulting amplitude into the vector and the tensor part

$$t_\lambda = i(\vec{A} \cdot \vec{\sigma}_{N\Delta}) + \sqrt{5} \left\{ A^{[2]} \otimes \sigma_{N\Delta}^{[2]} \right\}^{[0]} , \quad (8)$$

where the spin operator

$$\sigma_{N\Delta}^{[2]} \equiv \left\{ \sigma_N^{[1]} \otimes \sigma_{N\Delta}^{[1]} \right\}^{[2]} \quad (9)$$

has the reduced matrix element

$$\langle \frac{1}{2} \| \sigma_{N\Delta}^{[2]} \| \frac{3}{2} \rangle = -\sqrt{10}. \quad (10)$$

The quantities  $\vec{A}$  and  $A_\mu^{[2]}$  defined by (8) are functions of  $\vec{p}_N$  and  $\vec{p}_\Delta$  as well as the photon polarization vector  $\varepsilon_\lambda$  ( $\lambda=\pm 1$ ). After straightforward manipulation we find

$$\begin{aligned} \vec{A} &= -\sqrt{2} \frac{ef_\Delta}{m_\pi} \left\{ \vec{\varepsilon}_\lambda + F_\pi(t) \frac{2(\vec{q} - \vec{k})(\vec{q} \cdot \vec{\varepsilon}_\lambda)}{t - m_\pi^2} \right. \\ &+ \vec{q}_{\pi N} \left( \frac{e_\Delta(\vec{p}_\Delta \cdot \vec{\varepsilon}_\lambda)}{M_\Delta(E_\Delta + E_\gamma - E'_\Delta + \frac{i}{2}\Gamma_\Delta)} + \frac{e_N(\vec{p}_N \cdot \vec{\varepsilon}_\lambda)}{M_N(E_\Delta - E_\pi - E'_N)} \right) \\ &- \left. [\vec{q}_{\pi N} \times [\vec{k} \times \vec{\varepsilon}_\lambda]] \left( \frac{5\mu_\Delta}{4M_\Delta(E_\Delta + E_\gamma - E'_\Delta + \frac{i}{2}\Gamma_\Delta)} + \frac{\mu_N}{4M_N(E_\Delta - E_\pi - E'_N)} \right) \right\} \end{aligned} \quad (11)$$

$$\begin{aligned} A_\mu^{[2]} &= \sqrt{2} \frac{ef_\Delta}{m_\pi} \left\{ [\vec{k} \times \vec{\varepsilon}_\lambda]^{[1]} \otimes q_{\pi N}^{[1]} \right\}_\mu^{[2]} \\ &\times \left( \frac{\mu_\Delta}{2M_\Delta(E_\Delta + E_\gamma - E'_\Delta + \frac{i}{2}\Gamma_\Delta)} + \frac{\mu_N}{2M_N(E_\Delta - E_\pi - E'_N)} \right). \end{aligned} \quad (12)$$

Here  $E'_N = M_N + (\vec{p}_\Delta - \vec{q})^2/2M_N$  and  $E'_\Delta = M_\Delta + (\vec{p}_\Delta + \vec{k})^2/2M_\Delta$  are the energies of intermediate nucleon and delta and  $t = (E_\gamma - E_\pi)^2 - (\vec{k} - \vec{q})^2$ . We use the energy dependent resonance width

$$\Gamma_\Delta(W) = 115 \left( \frac{q_{\pi N}}{q_\Delta} \right)^3 \frac{M_\Delta}{W} \text{ MeV}, \quad (13)$$

with  $q_\Delta = 1.64 m_\pi$  and  $W$  being the  $\pi N$  invariant mass.

If we restrict ourselves to the c.m. system, the formal structure of the amplitude becomes similar to that for  $\gamma N \rightarrow \pi N$  process written in CGLN form [7]

$$\begin{aligned} t_\lambda &= iF_1(\vec{\sigma}_{N\Delta} \cdot \vec{\varepsilon}_\lambda) + F_2(\vec{\sigma}_N \cdot [\hat{k} \times \vec{\varepsilon}_\lambda])(\vec{\sigma}_{N\Delta} \cdot \hat{q}) \\ &+ iF_3(\vec{\sigma}_{N\Delta} \cdot \hat{k})(\hat{q} \cdot \vec{\varepsilon}_\lambda) + iF_4(\vec{\sigma}_{N\Delta} \cdot \hat{q})(\hat{q} \cdot \vec{\varepsilon}_\lambda), \end{aligned} \quad (14)$$

with  $\hat{p} \equiv \vec{p}/p$ . The amplitudes  $F_i$  read

$$\begin{aligned} F_1 &= -\sqrt{2} \frac{ef_\Delta}{m_\pi} \left[ 1 + \frac{\mu_\Delta(\vec{k} \cdot \vec{q})}{M_\Delta(E_\Delta + E_\gamma - E'_\Delta + \frac{i}{2}\Gamma_\Delta)} \right], \\ F_2 &= \sqrt{2} \frac{ef_\Delta}{m_\pi} kq \left[ \frac{\mu_\Delta}{2M_\Delta(E_\Delta + E_\gamma - E'_\Delta + \frac{i}{2}\Gamma_\Delta)} + \frac{\mu_N}{2M_N(E_\Delta - E_\pi - E'_N)} \right], \\ F_3 &= \sqrt{2} \frac{ef_\Delta}{m_\pi} kq \left[ \frac{2F_\pi(t)}{t - m_\pi^2} + \frac{\mu_\Delta}{2M_\Delta(E_\Delta + E_\gamma - E'_\Delta + \frac{i}{2}\Gamma_\Delta)} \right], \\ F_4 &= -\sqrt{2} \frac{ef_\Delta}{m_\pi} q^2 \left[ \frac{2F_\pi(t)}{t - m_\pi^2} - \frac{e_N}{2M_N(E_\Delta - E_\pi - E'_N)} \right]. \end{aligned} \quad (15)$$

Finally, the unpolarized differential c.m. cross section is related to the matrix element by

$$\frac{d\sigma}{d\Omega} = \frac{q}{k} \frac{M_\Delta M_N}{(4\pi)^2 W^2} \frac{1}{2} \sum_{\lambda=\pm 1} |\overline{t_\lambda}|^2, \quad (16)$$

where

$$\overline{|t_\lambda|^2} = \frac{1}{4} \sum_{m_\Delta m} |\langle \frac{1}{2}m|t_\lambda|\frac{3}{2}m_\Delta \rangle|^2 = \frac{1}{3} |\vec{A}|^2 + \frac{1}{2} \sum_\mu |A_\mu^{[2]}|^2. \quad (17)$$

Using the explicit expression for  $A_\mu^{[2]}$  (12), the last term in (17) may be written as

$$\begin{aligned} \sum_\mu |A_\mu^{[2]}|^2 &= 2 \left( \frac{ef_\Delta}{m_\pi} \right)^2 \left[ \frac{\mu_\Delta}{2M_\Delta(E_\Delta + E_\gamma - E'_\Delta + \frac{i}{2}\Gamma_\Delta))} + \frac{\mu_N}{2M_N(E_\Delta - E_\pi - E'_N)} \right]^2 \\ &\times \left[ k^2 q_{\pi N}^2 - \frac{1}{2} k^2 (\vec{q}_{\pi N} \cdot \vec{\varepsilon}_\lambda)^2 - \frac{1}{2} (\vec{q}_{\pi N} \cdot \vec{k})^2 - \frac{1}{3} (\vec{q}_{\pi N} \cdot [\vec{k} \times \vec{\varepsilon}_\lambda])^2 \right]. \end{aligned} \quad (18)$$

The calculated  $\gamma\Delta^{++} \rightarrow \pi^+ p$  cross section is presented in Fig.2, where in addition the separate contributions from the various terms depicted in Fig.1 are also shown. The distinguishing feature of the differential cross section (Fig.2a) is its localization in the backward hemisphere, which is due to the strong constructive interference between different terms in this region. Noteworthy also is the large contribution coming from the pion pole term (Fig.1c), which is much greater than that for the  $\gamma N \rightarrow \pi N$  amplitude. This observation is, however, of little consequence, since in physically realizable case of a bound delta, where the exchanged pion is far off-shell, the corresponding contribution turns out to be substantially reduced. The total cross section shown in Fig.2b has the shape peculiar to the exothermic reactions with divergence at the zero photon energy. This is also not the case for a bound delta, which, being far off-shell, does not produce any real pions, when  $E_\gamma \rightarrow 0$ . Thus, we conclude that the single particle cross section will be strongly affected, when implementing the elementary amplitude into the nucleus.

We proceed to discuss the application of our model for the  $\gamma\Delta^{++} \rightarrow \pi^+ p$  process to the nuclear reactions  $A(\gamma, \pi^+ p)$ . In order to connect all elementary ingredients with  $\Delta$ 's dynamics in nuclear medium, we employ here the standard impulse approximation as well as the closure relation  $\sum_f |f\rangle\langle f| = 1$  to sum over the states of residual nucleus. This approach yields for the lab cross section

$$\frac{d^3\sigma}{dT_\pi d\Omega_\pi d\Omega_p} = \frac{M_f M_N q p_N f_\pi(T_\pi) f_p(T_p)}{4(2\pi)^5 E_\gamma \left| E_f + E_N(1 - \vec{p}_N \cdot (\vec{k} - \vec{q})/p_N^2) \right|} \rho_{\Delta^{++}}(\vec{p}_\Delta) \frac{1}{2} \sum_{\lambda=\pm 1} \overline{|t_\lambda|^2}. \quad (19)$$

Here  $T_\pi$  and  $T_p$  stand for the pion and proton kinetic energy. The residual nuclear system is assumed to be  ${}^{11}Be$ (g.s.) with the mass  $M_f$  and the total energy  $E_f$ . The function  $\rho_{\Delta^{++}}(\vec{p}_\Delta)$  describes the distribution of bound deltas in terms of their momentum  $\vec{p}_\Delta$ . It is normalised as

$$\int \rho_{\Delta^{++}}(\vec{p}) \frac{d^3p}{(2\pi)^3} = \frac{N_\Delta}{4}, \quad (20)$$

where  $N_\Delta$  is the number of deltas in the target nucleus. In the actual calculation we use

$$\rho_{\Delta^{++}}(\vec{p}_\Delta) = 4 \cdot \frac{4}{3} \pi R^3 n(p_\Delta), \quad (21)$$

where  $R = 3.2$  fm is the square-well radius of  ${}^{12}C$  and the function  $n(p_\Delta)$  has a meaning of the  $\Delta$ 's occupation number inside the nuclear matter. The factor 4 in (20) accounts for the

spin magnetic number degeneracy. For the  $n(p_\Delta)$  we adopt the analysis of Ref.[8], which gives for the  $\Delta$  admixture in nuclear matter the value of the order of 7% per nucleon.

The  $\Delta$  constituent involved in  $\pi^+p$  formation through the elementary amplitude  $t_\lambda$  in (19) is treated to be off-shell as determined by the energy and momentum conservation for the elementary vertex

$$\begin{aligned}\vec{p}_\Delta &= \vec{q} + \vec{p}_N - \vec{k}, \\ E_\Delta &= E_\pi + E_N - E_\gamma.\end{aligned}\quad (22)$$

It is significant, that the photon energy  $240 \text{ MeV} \leq E_\gamma \leq 400 \text{ MeV}$  considered in this work is in great part not enough to overcome the  $\Delta$  binding energy ( $E_B \approx 300 \text{ MeV}$ ). Consequently, the  $A(\gamma, \pi^+p)$  reactions discussed here are essentially the  $\Delta$  decay in nuclear environment, rather than real  $\Delta$  knock-out processes [3].

In order to take the absorption of emerging particles while propagating in nuclear medium into account, the attenuation factors  $f_\pi(T_\pi)$  and  $f_p(T_p)$  are inserted in (19). Assuming square-well approximation for the  $\pi^+$ -nucleus and  $p$ -nucleus optical potential, these factors have a simple analytical form [9]

$$f_\alpha(T_\alpha) = \frac{3l_\alpha}{4R} \left[ 1 - \frac{l_\alpha^2}{2R^2} \left\{ 1 - \left( 1 + \frac{2R}{l_\alpha} \right) e^{-\frac{2R}{l_\alpha}} \right\} \right], \quad (\alpha = \pi^+, p), \quad (23)$$

which is entirely determined by the mean free path  $l_\alpha(T_\alpha)$  of the corresponding particle in nuclear matter.

Now we compare our numerical results to the available data [4]. Following the experimental conditions of [4], the triple differential cross section was averaged over the angles  $50^\circ \leq \theta_\pi \leq 130^\circ$  and  $10^\circ \leq \theta_p \leq 150^\circ$ . It is seen from Fig.3 that our results for the  $^{12}C(\gamma, \pi^+p)$  cross section progressively underestimate the data with increasing photon energy. In Fig.4, where we show our calculation for the pion kinetic energy distribution, theoretical predictions agree roughly with the experimental cross section, when  $T_\pi \geq 80 \text{ MeV}$ . At that time, we can not reproduce relatively large values of the low-energy data.

We would like to note that our model yields a rather essential fraction of observed pion spectrum, especially for large energies. The calculated cross section has the same order of magnitude as that obtained within the VM approach, which attributes all  $\pi^+p$ -production events to the final state rescattering processes as mentioned previously. The results of VM calculation are also shown in Fig.4. One observes a strong difference in shape of pion energy spectrum predicted by two models. Whereas the VM cross section, which is expected to be governed mainly by the reaction phase space, is concentrated in the region of small  $T_\pi$  and falls off rapidly with increasing pion energy, our curve peaks at  $T_\pi = 90 \text{ MeV}$  and shows only a little value of the low-energy spectrum.

It is necessary to give some remarks in respect to the validity of our calculation. As far as we are concerned with the averaged values of the exclusive cross section, our results are

expected to be not very sensitive to the choice of the model ingredients, such as the shape of  $\Delta$ 's momentum distribution as well as probably more accurate inclusion of pion and proton distortion in the final state, etc. Thus, we hope that possible changes brought about by more sophisticated models will hardly be significant. However, some effects can markedly modify our quantitative conclusions.

First there is a large uncertainty in the choice of  $\Delta$  magnetic moment  $\mu_{\Delta^{++}}$ . The value  $\mu_{\Delta^{++}} = -2.3$  n.m. [6] used here differs greatly from  $\mu_{\Delta^{++}} = 5.6$  n.m. predicted by simple SU(6) model. One can also mention relatively large value  $\mu_{\Delta^{++}} = 4.2 \pm 0.5$  n.m. obtained from the  $\pi^+p \rightarrow \pi^+p\gamma$  analysis [11]. Regarding  $\mu_{\Delta^{++}}$  as free parameter, we obtain a strong increase of the cross section by about a factor of 5, when varying the magnetic moment in the range from  $-2.3$  to  $5.6$  n.m. Thus, it is very important to know the precise value of  $\mu_{\Delta^{++}}$  for an accurate calculation.

Another probable modifications will come from the more refined study of the role of  $\Delta$  isobar configurations in  $^{12}C$  ground state. Indeed, the number of deltas of about 0.07 per nucleon given by the model [8], which we adopt here, is relatively high as compared to  $N_\Delta \approx 3.7\%$  [10] for the nuclear matter as well as to those predicted for finite nuclei (generally less than 4% [2]).

In conclusion, the aim of this paper is to attract the attention to the  $A(\gamma, \pi^+p)$  reactions, which offer unique possibilities for testing and extending our knowledge about  $\Delta$  degrees of freedom in nuclei. Our results for  $^{12}C(\gamma, \pi^+p)$  reaction are in rough agreement with the existing data [4]. The calculated cross section is comparable to that given by the FSI mechanism regarded by VM model [5]. Coming back to the Fig.4, one can speculate that the observed cross section is filled by both channels, although we recall that the uncertainty in the model parameters makes our quantitative conclusion rather ambiguous. In this respect, it is important to point out that more usefull information on the role of virtual deltas in  $A(\gamma, \pi^+p)$  reactions may be obtained from the true exclusive data (not averaged over a wide range of angles as presented in [4]). Such measurements make it possible to separate the FSI background from the  $\Delta^{++}(\gamma, \pi^+p)$  events. Experiments along these lines are in progress at Tomsk synchrotron. To complete this discussion, we would like to note that the  $A(\gamma, \pi^+p)$  measurements on lightest nuclei, such as deuteron and  $^3H$ , are also highly desirable. In this case, the FSI contribution is assumed to be of minor importance and the information about  $\Delta^{++}(\gamma, \pi^+p)$  amplitude may be interpreted unambiguously. What is more, minimal number of nucleons allows a carefull microscopic treatment of these processes.

This work was supported in part by the Russian Foundation for Fundamental Research under Contract No. 96-02 16742-a.

## References

- [1] A.M. Green, Rep.Progr.Phys. **39** (1976) 1109
- [2] H.J. Weber, H. Arenhövel, Phys.Rep. **36** (1978) 277
- [3] S.B. Gerasimov, ZhETF Pis.Red. **14** (1971) 385 (JETP Lett. 14 (1971) 260)
- [4] M. Liang, D. Branford, T. Davinson *et al.*, Phys.Lett. **B411** (1997) 244
- [5] R. Carrasco, E. Oset, Nucl.Phys. A536 (1992) 445
- [6] Y.A. Chao, R.K.P. Zia, Nuovo Cimento **A19** (1974) 651
- [7] G.F. Chew, M.L. Goldberger, F.E. Low, Y. Nambu, Phys. Rev. **106** (1957) 1345
- [8] R. Cenni, F. Conte, U. Lorenzini, Phys.Rev. **C39** (1989) 1588
- [9] J.-M. Laget, Nucl.Phys. **A194** (1972) 81
- [10] B.D. Day, R. Coester, Phys. Rev. **C13** (1976) 1720
- [11] D. Lin, R.K. Liou, Phys. Rev. **C43** (1991) 930

### Figure captions

**FIG.1** Diagrams for the  $\gamma\Delta^{++} \rightarrow \pi^+ p$  amplitude used in the present calculation: s-channel term (a), u-channel term (b), pion pole term (c), seagull term (d).

**FIG.2** (a) Angular distribution for the  $\gamma\Delta^{++} \rightarrow \pi^+ p$  reaction in c.m. system. The curves present the contributions from different terms depicted in Fig.1: full calculation (solid), s-channel term (dashed), u-channel term (dash-dotted), pion pole term (dotted), seagull term (dash-double dotted).

(b) Total cross section for the  $\gamma\Delta^{++} \rightarrow \pi^+ p$  reaction.

**FIG.3** Triple differential cross section for the  $^{12}C(\gamma, \pi^+ p)$  reaction versus photon energy, averaged over the angles of emitted particles  $50^\circ \leq \theta_\pi \leq 130^\circ$  and  $10^\circ \leq \theta_p \leq 150^\circ$ . The pion and proton thresholds are set at  $T_\pi = 30$  MeV and  $T_p = 50$  MeV. The data are taken from [4].

**FIG.4** Pion kinetic energy distribution for the  $^{12}C(\gamma, \pi^+ p)$  reaction. Step line is the VM calculation [5]. The data are from [4].

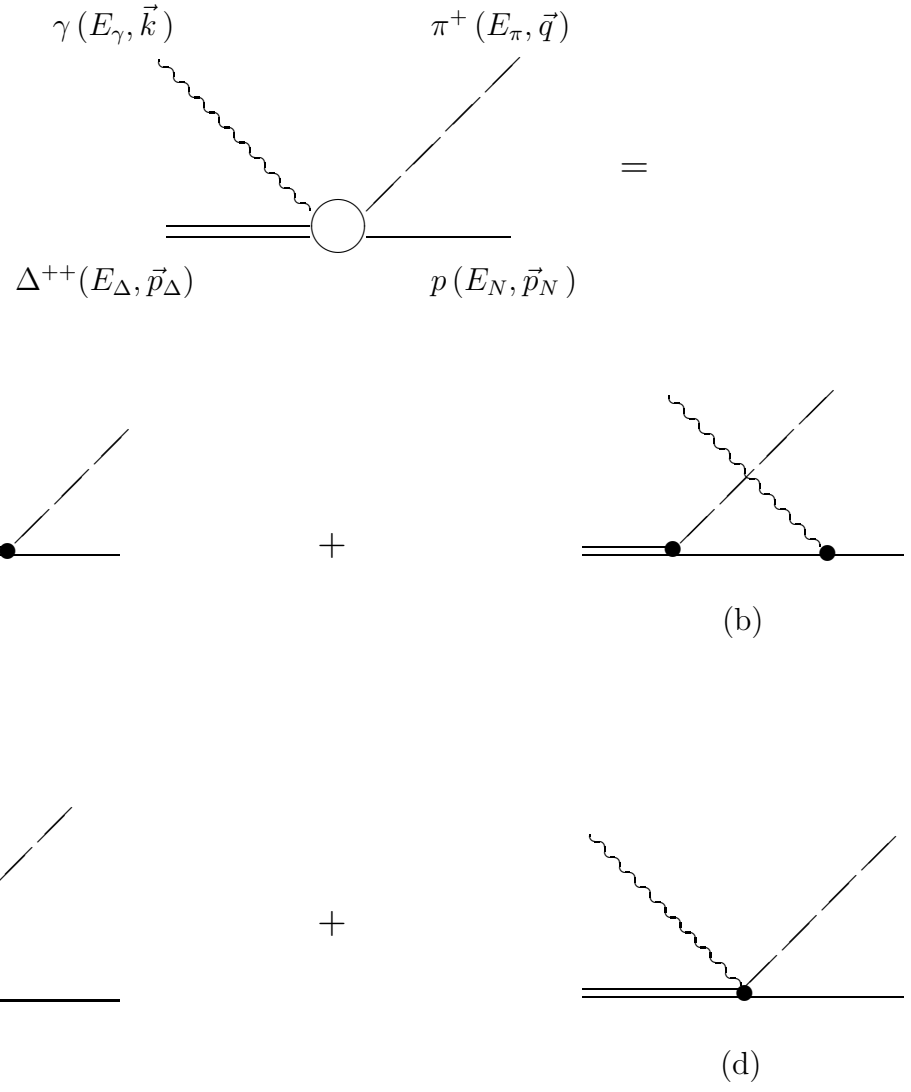


Figure 1.